Indomethacin treatment prevents high fat diet-induced obesity and insulin resistance but not glucose intolerance in C57BL/6J mice.

Even Fjære, Ulrike L Aune, Kristin Røen, Alison H Keenan, Tao Ma, Kamil Borkowski, David M Kristensen, Guy W Novotny, Thomas Mandrup-Poulsen, Brian D Hudson, et al.

▶ **To cite this version:**

Even Fjære, Ulrike L Aune, Kristin Røen, Alison H Keenan, Tao Ma, et al.. Indomethacin treatment prevents high fat diet-induced obesity and insulin resistance but not glucose intolerance in C57BL/6J mice.. Journal of Biological Chemistry, 2014, 289 (23), pp.16032-45. 10.1074/jbc.M113.525220 . hal-01074835

HAL Id: hal-01074835

https://univ-rennes.hal.science/hal-01074835

Submitted on 3 Nov 2014

HAL is a multi-disciplinary open access archive for the deposit and dissemination of scientific research documents, whether they are published or not. The documents may come from teaching and research institutions in France or abroad, or from public or private research centers.

L'archive ouverte pluridisciplinaire **HAL**, est destinée au dépôt et à la diffusion de documents scientifiques de niveau recherche, publiés ou non, émanant des établissements d'enseignement et de recherche français ou étrangers, des laboratoires publics ou privés.

Indomethacin treatment prevents high-fat diet-induced obesity and insulin resistance, but not glucose intolerance in C57BL/6J mice

Even Fjære[1,2], Ulrike L. Aune[1,2], Kristin Røen[1], Alison H. Keenan[1,3], Tao Ma[1], Kamil Borkowsky[1], David M. Kristensen[5,6], Guy W. Novotny[7], Thomas Mandrup-Poulsen[7,8], Brian D. Hudson[9], Graeme Milligan[9], Yannan Xi[3], John W. Newman[3,10], Fawaz G. Haj[3,4], Bjørn Liaset[2], Karsten Kristiansen[1,*], and Lise Madsen[1,2,*]

[1]Department of Biology, University of Copenhagen, Copenhagen, Denmark. [2]National Institute of Nutrition and Seafood Research, Bergen, Norway. [3]Department of Nutrition and [4]Internal Medicine, University of California, Davis, USA. [5]Institut National de la Santé et de la Recherche Médicale (INSERM) U1085-IRSET, Université de Rennes 1, Rennes, France. [6]Department of Biomedical Sciences, Faculty of Health Sciences, University of Copenhagen, Copenhagen, Denmark. [7]Section for Endocrinological Research, Department of Biomedical Sciences, University of Copenhagen, Copenhagen, Denmark. [8]Department of Molecular Medicine and Surgery, Karolinska Institute, Stockholm, Sweden. [9]Institute of Molecular, Cell and Systems Biology, University of Glasgow, Scotland, United Kingdom. [10]USDA/ARS Western Human Nutrition Research Center, California, USA.

Running title: Cyclooxygenase inhibition and regulation of glucose homeostasis.

* Correspondence to: Lise Madsen, National Institute of Nutrition and Seafood Research, P.O.BOX 2029 Nordnes, N-5817 Bergen, Norway. Fax: +47 5590 5299; Phone: +47 4147 6177; Email: lise.madsen@nifes.no or Karsten Kristiansen, Department of Biology, University of Copenhagen, Ole Maaløes Vej 5, DK-2200 Copenhagen N, Denmark. Fax: +45 3532 2128; Phone: +45 3532 4443; Email: kk@bio.ku.dk

Keywords: Adipose tissue; Cyclooxygenases (COXs) pathway; Cyclooxygenase inhibitors; G-protein coupled receptor; Glucose intolerance; Insulin resistance; Insulin secretion

Background: Obesity-associated insulin resistance is linked to inflammation.
Results: Indomethacin, an anti-inflammatory cyclooxygenase inhibitor, prevented diet-induced obesity and overall peripheral insulin resistance, but mice became glucose intolerant with sustained hepatic glucose output. Selective activation of the fatty acid receptor GPR40 in the presence of indomethacin impaired glucose-stimulated insulin secretion, in part explaining the interaction between intake of a high fat obesogenic diet and indomethacin.
Conclusion: Inhibition of cyclooxygenase activity alters the metabolic consequences of an obesogenic diet.
Significance: Intake of anti-inflammatory cyclooxygenase inhibitors may impair glucose tolerance.

ABSTRACT

Chronic low-grade inflammation is closely linked to obesity-associated insulin resistance. To examine how administration of the anti-inflammatory compound indomethacin, a general cyclooxygenase inhibitor, affected obesity development and insulin sensitivity, we fed obesity-prone male C57BL/6J mice a high fat/high sucrose (HF/HS) diet or a regular diet supplemented or not with indomethacin (+/-INDO) for 7 weeks. Development of obesity, insulin resistance and glucose intolerance was monitored, and the effect of indomethacin on glucose stimulated insulin-secretion (GSIS) was measured *in vivo*, and *in vitro* using MIN6 β-cells. We found that supplementation with indomethacin prevented HF/HS-induced obesity and diet-induced changes in systemic insulin sensitivity. Thus, HF/HS+INDO fed mice

remained insulin sensitive. However, mice fed HF/HS+INDO, exhibited pronounced glucose intolerance. Hepatic glucose output was significantly increased. Indomethacin had no effect on adipose tissue mass, glucose tolerance or GSIS when included in a regular diet. Indomethacin administration to obese mice did not reduce adipose tissue mass, and the compensatory increase in GSIS observed in obese mice was not affected by treatment with indomethacin. We demonstrate that indomethacin did not inhibit GSIS *per se*, but activation of GPR40 in the presence of indomethacin inhibited glucose-dependent insulin secretion in MIN6 cells. We conclude that constitutive high hepatic glucose output combined with impaired GSIS in response to activation of GPR40-dependent signaling in the HF/HS+INDO fed mice contributed to the impaired glucose clearance during a glucose challenge, and that the resulting lower levels of plasma insulin prevented the obesogenic action of the HF/HS diet.

INTRODUCTION

Chronic low-grade inflammation is a key factor underlying obesity-associated insulin resistance (1,2). Cyclooxygenase (COX) derived prostaglandins (PGs) are mediators of tissue inflammation, but may also influence insulin secretion as well as adipocyte differentiation and function. The relationship between PGs and insulin secretion is complex and apparently conflicting results have been reported. Increased levels of PGs have been associated with impaired β-cell function (3). PGE_2 was reported to reduce glucose-stimulated insulin secretion (GSIS), and accordingly, administration of COX inhibitors increased GSIS and improved glucose disposal (4). By contrast, administration of the general COX inhibitor, indomethacin, a commonly used nonsteroidal anti-inflammatory drug (NSAID), has been shown to decrease insulin secretion in T2DM patients (5), and to lower glucose-stimulated acute insulin response (6).

PGs have both pro- and anti-obesogenic properties (7). Others and we have shown that both diet- and cold-induced appearance of brown-like adipocytes, termed “brite” or “beige” adipocytes in white adipose tissues requires COX expression and activity (8,9). Thus, in the apparently obesity-resistant Sv129 mouse strain, treatment with indomethacin, attenuated diet-induced expression of uncoupling protein 1 (*Ucp1*) in inguinal white adipose tissue (iWAT), thereby promoting the development of diet-induced obesity (8).

The present study was designed to examine how indomethacin affected diet-induced obesity and the associated metabolic disorders in obesity prone male C57BL/6J mice. In sharp contrast to the effect in Sv129 mice (8), indomethacin treatment prevented the obesogenic effects of a high fat/high sucrose (HF/HS) diet in C57BL/6J mice. Our results reveal an interesting and complex phenotype of HF/HS fed C57BL/6J mice treated with indomethacin (HF/HS+INDO). Compared with C57BL/6J mice fed a HF/HS diet, mice fed a HF/HS+INDO diet were lean and remained insulin sensitive, yet they became glucose intolerant; a feature likely associated with impaired regulation of hepatic gluconeogenesis and impaired compensatory upregulation of pancreatic insulin secretion.

EXPERIMENTAL PROCEDURES

Mouse care and maintenance. Eight week old male C57BL/6JBomTac mice (Taconic, Ejby, Denmark) were acclimated for 1 week under thermoneutral conditions (28-30°C) with a 12-hour light and dark cycle. Mice were housed individually. Two sets of mice were assigned to three groups (n=9/group) and fed a low fat (LF), regular diet (RD) (ssniff EF R/M Control, Germany), a HF/HS diet, (ssniff S8672-E056 EF, Germany) or a HF/HS diet supplemented with indomethacin (16 mg/kg) (Sigma-Aldrich, Norway) for 7 weeks. A third set of mice were fed a HF/HS diet for 10 weeks before they were fed the HF/HS diet supplemented with indomethacin. A fourth set of mice was given saline or indomethacin (2.5 mg/kg body mass), dissolved in saline, by gavage after 5 hours fasting and 1 hour prior to glucose administration. In all experiments, food intake was recorded three times a week, and body weight once per week. All animal experiments were approved by the National State Board of Biological Experiments with Living Animals (Norway and Denmark).

Glucose, insulin and pyruvate tolerance test. For glucose tolerance test (GTT) and pyruvate

tolerance test (PTT) the animals were injected i.p. after 6 hours of fasting with 2 g glucose/kg body weight or 2 g sodium pyruvate (Sigma-Aldrich)/kg body weight (10). For insulin tolerance test (ITT) 0.75 U human insulin (Actrapid, Denmark)/kg body weight was injected i.p. in the fed state. For all tests, blood was collected from the tail vein of conscious animals and blood glucose was measured using a glucometer (Ascensia Contour, Bayer, Norway) at baseline and at the indicated times.

Glucose-stimulated insulin secretion. Mice fasted for 3 hours were injected i.p. with 3 g glucose/kg body weight. Blood (30µl) was collected from the tail vein at baseline and 2, 5 and 10 minutes after glucose injection.

Indirect calorimetry. After 6 weeks on their respective diets and a 24 hour acclimatization period, O_2 and CO_2 gas exchange measurements were obtained for a 24 hour period from each mouse, using the open circuit chambers of the Labmaster system (TSE Systems GmbH, Germany) (11).

Termination and tissue harvest. Mice were anesthetized with isoflurane (Isoba-vet, Schering-Plough, Denmark) and euthanized by cardiac puncture. Blood samples were collected in tubes containing EDTA anticoagulant. Organs were immediately dissected, weighed, and flash-frozen in liquid nitrogen and stored at -80°C.

Histology examinations. Paraffin embedded sections of eWAT and iWAT were stained with haematoxylin and eosin, and analyzed as previously described (12). Sections of pancreatic tissue were stained for insulin, and pancreatic islet and section sizes were analyzed (13). Immunohistological detection of UCP1 positive multilocular cells was performed by an avidin-biotin peroxidase method. After deparaffination and rehydration, 5 µm sections were processed through citrate buffer (pH6), 2x15 min (95°C). Sections were transferred to 0.3% hydrogen peroxide in methanol (30 min), before incubation with 10% goat serum (30 min), and incubation with primary antibody 1:4000 in PBS (goat serum 1%) over night (4°C). Secondary antibody 1:200 was applied for 1 hour and incubation with the ABC complex (Vectastain ABC kit, Vector Laboratories), as described by the manufacturer. *DAB* (3,3'-diaminobenzidine) (Vector Laboratories, Burlingame, CA) substrate kit was applied, before counterstaining with hematoxylin and mounting. F4/80 immunohistological detection of macrophages in adipose tissue was performed by using the F4/80 sc-52664 (BM8) antibody and ImmunoCrus rat ABC staining system sc-2019 as described by the manufacturer (Santa Crus Biotechnology, Texas, USA).

Cell culture. MIN6 cells were cultured at 37°C in a humidified atmosphere containing 5% CO2 in RPMI1640 media with GlutaMAX supplemented with 10% [vol./vol.] FCS, 100 U/ml penicillin, 100 µg/ml streptomycin (all from Invitrogen/Gibco, Denmark) and 50 µmol/l β-mercaptoethanol (Sigma) together with vehicle (DMSO) or 1µM indomethacin. After 48 hours, cells were washed and incubated for 30 min in Krebs-Ringer-bicarbonate buffer (KRB) containing 135 mM NaCl, 3.6 mM KCl, 0.5 mM NaH_2PO_4, 2 mM $NaHCO_3$, 0.5 mM $MgCl_2$, 1.5 mM $CaCl_2$, 10 mM HEPES, 2.8 mM glucose and 0.05% BSA, together with either indomethacin or vehicle. The buffer was replaced with 0.5 ml fresh KRB containing either vehicle, indomethacin, 10 µM TUG469, a synthetic GPR40 agonist (14) or a combination. Insulin release was measured after 1 hour.

MIN6 viability measurements over 48 hours were performed using the xCELLigence platform (Roche Diagnostics) (15), with indomethacin or vehicle (DMSO) added after 24 hours of growth.

Bioluminescence Resonance Energy Transfer (BRET) based β-arrestin-2 interaction assay. HEK293T cells were transiently transfected using polyethylenimine with constructs encoding mouse GPR40 tagged at its carboxy terminal with enhanced yellow fluorescence protein and β-arrestin-2 fused with Renilla luciferase. The ability of TUG469 and indomethacin to affect interaction between the mouse GPR40 and β-arrestin-2 constructs was assessed using the BRET based method (16). The resulting concentration-response data were fit to 3-parameter sigmoid curves using

GraphPad Prism v 5.0 (GraphPad Software, Inc., San Diego, CA, USA).

Plasma measurements. Glycerol, NEFA, plasma glucose, alanine aminotransferase (ALT) and aspartate transaminase (AST) concentrations in plasma were analyzed with commercially available enzymatic kits (Dialab, Vienna, Austria) using an autoanalyzer (MaxMat SA, Montpellier, France). Insulin Mouse Ultrasensitive ELISA kit (DRG Diagnostics GmbH, Germany) was used for quantitative determination of insulin in plasma. Homeostasis model assessment of insulin resistance (HOMA-IR) was calculated from fasting insulin and glucose concentrations using the formula: plasma glucose (mmol/l)×plasma insulin (µU/ml)/22.5 (17). QUICKI was calculated using the formula: 1/(log(fasting insulin µU/ml) + log(fasting glucose mg/dl)) (18).

Real time RT-qPCR. RNA was extracted from tissue, cDNA synthesized and gene expression measured as described (19).

Tissue lipid extraction and lipid class analysis. Total lipid was extracted from liver and muscle samples with chloroform:methanol, 2:1 (v/v) and quantified on a Camaq High performance thin layer chromatography (HPTLC) system and separated on HPTLC silica gel (20). Total lipid was extracted from feces and quantified in samples from 48 hours collection (12) after 6 weeks of treatment with the respective diets.

Plasma oxylipins. Plasma samples were extracted using Oasis HLB solid phase extraction cartridges (Waters Corp Inc, Milford MA, USA) as previously described (21). Analytes were eluted with methanol and ethyl acetate into 6µl glycerol, subjected to vacuum evaporation, and the resulting glycerol plug was stored at -80°C. Prior to analysis, samples were reconstituted in methanol containing 100nM of each internal standard 1-cyclohexyl-ureido-3-dodecanoic acid and 1-phenylurea-3-hexanoic acid (Sigma-Aldrich), followed by filtration at 0.1µm and analysis by UPLC-MS/MS. The analytes were separated using a reverse phase solvent gradient on a 2.1 x 150mm, 1.7µm Acquity BEH column, ionized by negative mode electrospray ionization and detected by multi-reaction monitoring mode on an ABI 4000QTRAP (ABSciex, Foster City, CA, USA) triple quadrupole mass spectrometer (22).

Statistics. All results are shown as mean ± SEM unless otherwise indicated. Statistical analyses of physiological and gene expression data were performed with GraphPad Prism v 5.0 (GraphPad Software, Inc.), and Dixon's Q-test was used to screen for outliers. One-way ANOVA was used to compare differences between the experimental groups, followed by Fisher`s LSD test unless otherwise indicated. A significance level of $P \leq 0.05$ was used for all tests. Statistical significances are denoted with stars; * $P \leq 0.05$, ** $P \leq 0.01$, *** $P \leq 0.001$.

RESULTS

Indomethacin prevents diet-induced obesity in C57BL/6J mice. Obesity-prone C57BL/6J mice were fed a HF/HS diet with or without indomethacin. Mice fed a HF/HS diet had increased weight gain, increased white adipose tissue (WAT) and liver masses compared with mice fed RD, whereas these increases were prevented in mice fed HF/HS+INDO (Fig. 1A, B, C and D). No differences in weights of iBAT (Fig. 1E) or of the skeletal muscles, tibialis anterior or soleus were observed (data not shown).

Indomethacin reduces feed efficiency. To confirm that the reduced obesity in HF/HS+INDO fed mice was not simply due to reduced energy intake, feed intake was monitored. Energy intake was comparable between HF/HS and HF/HS+INDO fed mice (Fig. 1F), and thus, indomethacin supplementation reduced feed efficiency (Fig. 1G). As indomethacin has been reported to decrease bile acid secretion, with a possible effect on fat absorption (23,24), the apparent fat digestibility was calculated. Indomethacin treatment did not decrease fat absorption compared with mice fed the HF/HS diet, but both HF/HS fed groups had increased fat absorption compared to RD fed mice (Fig. 1H).

The reduced feed efficiency and higher percentage weight loss after 12 hours starvation (Fig. 1I) in HF/HS+INDO fed mice compared with HF/HS fed mice could indicate increased metabolic activity and therefore

indirect calorimetry measurements were performed. O_2 consumption, CO_2 production and the respiratory exchange ratio (RER) were similar in the HF/HS and HF/HS+INDO fed groups. No significant difference was observed between HF/HS and HF/HS+INDO, but O_2 consumption, CO_2 production and the respiratory exchange ratio (RER) were significantly lower compared to the RD fed mice (Fig. 2A-C). Unexpectedly, expression of *Ucp1* in iWAT was higher in mice fed HF/HS+INDO than in mice fed HF/HS, but comparable in their iBAT and eWAT (Fig. 2D). Expression of other brown adipocyte markers was not significantly different (Fig. 2E and F). To evaluate if the increased mRNA expression of *Ucp1* in iWAT was accompanied with UCP1 positive multilocular cells, immunohistochemical (IHC) analyses of in both eWAT and iWAT were performed. The IHC staining revealed no induction of UCP1 positive cells in eWAT, irrespective of diet group, however, in agreement with the mRNA levels of *Ucp1* a minute induction was observed in iWAT of mice fed HF/HS+INDO (Fig. 2G). Despite a significant induction of *Ucp1* within iWAT, the relative expression is extremely low compared the expression seen in iWAT of obesity-resistant mouse strains. Thus, we conclude that the low level of UCP1 in iWAT in mice fed the HF/HS+INDO diet is insufficient to explain energy balance and the observed differences in body weight and fat mass.

Indomethacin increases plasma glycerol and NEFA in the fasted state. The reduced feed efficiency in HF/HS+INDO compared with HF/HS fed mice was not associated with increased plasma levels of AST or ALT. (Fig. 2H), indicating that the low dose of indomethacin in the diet did not cause liver injury (Fig. 2H). PGs, PGE_2 in particular, inhibit lipolysis (25). Hence, we asked if treatment with indomethacin would affect lipolysis. In the fed state, glycerol and NEFA levels were comparable in all groups (Fig. 2I and J). However, in the fasted state, both glycerol and NEFA levels were higher in HF/HS+INDO than in HF/HS fed mice (Fig. 2I and J), indicating increased mobilization of fat from adipose tissue in indomethacin treated mice.. This effect might reflect a more unabated ability of the increased levels of cAMP to increase lipolysis during fasting in the absence of inhibitory PGE_2.

Indomethacin prevents diet-induced hypertrophy and attenuates expression of inflammatory markers in iWAT. As hypertrophy is associated with increased infiltration of macrophages and low grade inflammation (26), histological examinations and gene expression analyses of macrophage infiltration markers were performed. HF/HS diet-induced hypertrophy of eWAT and iWAT was prevented by indomethacin treatment (Fig. 3A). Expression of markers for macrophage infiltration and inflammation in eWAT was not increased significantly in response to HF/HS feeding for 7 weeks, except for Chemokine ligand 2 (*Ccl2*) (Fig. 3B-E). On the other hand, expression of *Cd68*, and *Ccl2* in iWAT was significantly reduced by an HF/HS diet with indomethacin supplementation. Expression of *Emr1* (P= 0.08) also tended to be reduced in HF/HS+INDO fed mice (Fig. 3F-I). .

Macrophage infiltration in AT depots was evaluated by IHC staining with F4/80 antibody. The evaluation of F4/80 positive macrophages showed infiltration in the AT of mice given LF, HF/HS and HF/HS+INDO, and is in agreement with the mRNA expression. Despite no significant differences in the number of F4/80 positive macrophages per 100 counted adipocytes (eWAT: RD= 43.9 ± 6.2, HF/HS= 58.7 ± 5.0 and HF/HS+INDO = 50.1 ± 6.8, and iWAT: RD = 31.1±6.5, HF/HS = 34.4±4.8 and HF/HS+INDO = 27.7±2.4), IHC revealed that the formation of crown-like structures (CLSs) was only observed in the HF/HS-diet group (Fig. 3J).

Plasma oxylipin profiles in mice fed HF/HS and HF/HS+INDO. To ascertain the efficacy of indomethacin treatment and obtain an overview of changes in plasma eicosanoids, plasma non-esterified oxylipin profiles were assessed. Cyclooxygenase-dependent metabolite levels in plasma were significantly reduced in mice given HF/HS+INDO compared with mice given a HF/HS diet. The levels of prostaglandins 6-keto $PGF_{1\alpha}$, PGD_2 as well as thromboxane B2 (TXB2) were significantly reduced by indomethacin supplementation, suggesting impacts on both

COX1 and COX2 dependent metabolism (Table. 1).

Indomethacin supplementation attenuates HF/HS-induced diacylglycerol and triacylglycerol accumulation in liver and skeletal muscle. To investigate if the reduced adipose tissue mass in HF/HS+INDO fed mice was associated with increased ectopic fat accumulation, different lipid classes were quantified in liver and muscle tissue. Indomethacin attenuated HF/HS -induced accumulation of triacylglycerol (TAG) and diacylglycerol (DAG) in both liver and tibialis anterior muscle (Fig. 4A-D). The levels of phospholipids were not affected in liver or muscle by any diet (data not shown).

Indomethacin treatment attenuates HF/HS-induced whole-body insulin resistance. Diet-induced accumulation of DAG and TAG in liver and muscle is associated with reduced insulin sensitivity (27-29). Thus, we examined whether inclusion of indomethacin in the diet also prevented HF/HS-induced insulin resistance. Calculation of the HOMA-IR index, indicated reduced insulin sensitivity in HF/HS fed mice, whereas mice fed HF/HS+INDO exhibited comparable HOMA-IR and QUICKI to those of RD fed mice (Fig. 4E and F). Importantly, ITT demonstrated significantly reduced insulin sensitivity in HF/HS fed mice, whereas mice fed HF/HS+INDO exhibited insulin sensitivity comparable to that of mice fed RD (Fig. 4G).

Indomethacin does not prevent hyperglycemia and impaired glucose tolerance associated with a HF/HS diet. Despite being lean and insulin sensitive, HF/HS+INDO fed mice exhibited elevated levels of plasma glucose in the fed and fasted state compared with RD fed mice (Fig. 5A). Furthermore, HF/HS+INDO fed mice were as glucose intolerant as those fed HF/HS, indicating that HF/HS+INDO fed mice were unable to cope with the glucose challenge imposed by the GTT (Fig. 5B). Despite a reduction in glucose tolerance in mice given HF/HS+INDO, no compensatory enhancement of glucose-stimulated insulin secretion (GSIS) was observed 15 minutes after glucose injection compared to that observed in mice fed a HF/HS-diet, (Fig. 5C). To evaluate whether increased hepatic glucose output might contribute to the high plasma glucose values in HF/HS+INDO mice, a PTT was performed. Mice fed the HF/HS diet had increased blood glucose levels after a pyruvate injection compared with RD fed mice, and this was not attenuated by indomethacin (Fig. 5D). Expression of G6pc (Glucose-6-phosphatase) and Pck1 (Phosphoenolpyruvate carboxykinase 1) was significantly increased in both HF/HS and HF/HS+INDO treated mice, compared with mice fed a low fat RD (Fig. 5E and F).

Indomethacin prevents HF/HS-induced glucose-stimulated insulin secretion.
To further investigate the reduced glucose tolerance in HF/HS+INDO fed mice, glucose tolerance and GSIS were examined in a second set of mice after 1, 2 and 3 weeks of feeding. Interestingly, the HF/HS+INDO fed mice exhibited clear signs of glucose intolerance already after one week of feeding with no alterations in GSIS as measured 15 minutes after glucose injection and no significant difference in BW (Fig. 5G&H). After 3 weeks of feeding both the HF/HS and the HF/HS+INDO fed mice were markedly glucose intolerant, but only the HF/HS fed mice exhibited a compensatory increase in GSIS reflecting the insulin resistant state of these mice (Fig. 5K&L). This indicates that indomethacin exerted an early effect on glucose intolerance that temporally preceded changes in GSIS and increased glucose intolerance in the HF/HS fed mice. Moreover, these results suggest that indomethacin did not directly inhibit GSIS.
To establish whether indomethacin acutely affected glucose clearance and GSIS, RD fed mice were orally treated with a single dose of indomethacin. This treatment acutely impaired glucose disposal in spite of no significant impairment in GSIS (Fig. 6A-C). Neither glucose tolerance nor GSIS was affected by acute administration of indomethacin in obese, glucose intolerant HF/HS fed mice (Fig. 6D-F).

To evaluate if long term treatment with indomethacin was able to influence glucose tolerance and GSIS in the setting of a RD feeding, we fed mice RD+/-INDO, for 7 weeks. Body weight (data not shown) and WAT mass in RD+INDO fed mice were comparable to those fed RD (Fig. 6G). In this

context indomethacin supplementation did not lead to glucose intolerance (Fig. 6H) or alterations in GSIS (Fig. 6I).

Finally, we aimed to investigate if treatment with indomethacin could reverse elevated HF/HS-induced GSIS in obese and insulin resistant mice. To increase fat mass and reduced insulin sensitivity, C57BL/6J mice were fed a HF/HS-diet for 10 weeks; then a group was switched to HF/HS+INDO-diet and another maintained on HF/HS for 8 additional weeks. Mice fed a RD were used as a reference. No reduction in BW, feed efficiency, and lean- and fat mass was observed when obese mice were fed HF/HS+INDO (Fig. 6J-M). Furthermore, we observed no effect of INDO treatment regarding glucose tolerance and GSIS in already obese animals (Fig. 6N&O).

Indomethacin treatment combined with activation of GPR40 attenuates GSIS. To corroborate the notion that mice fed HF/HS+INDO failed to compensate for a sustained hepatic glucose production, insulin levels were measured in both the fasted and fed states and β-cell mass was quantified after 8 weeks of feeding. In spite of the marked glucose intolerance, the HF/HS diet-induced hyperinsulinemia in both the fasted and fed states was not observed in HF/HS+INDO fed mice (Fig. 7A). Quantification of pancreatic β-cell mass demonstrated no reduction in β-cell mass in the HF/HS fed mice (Fig. 7B). Evaluation of insulin secretion upon an i.p. injection of glucose demonstrated that insulin secretion in mice fed the HF/HS+INDO diet was comparable to the RD fed mice, whereas it was increased in the HF/HS fed mice (Fig. 7C). Fatty acid-dependent modulation of GSIS depends on both β-cell fatty acid metabolism and signaling via GPR40/FFA1 (30-32). To examine if indomethacin cell-autonomously modulated GSIS when GPR40/FFA1 was activated, we analyzed the effect of indomethacin on GSIS in the presence and absence of a synthetic GPR40 agonist, TUG469, in mouse MIN6 cells. No effect on cell survival and growth in response to treatment with up to 10 μM indomethacin was observed (Fig. 7 D) and indomethacin alone, did not impair GSIS in MIN6 cells. However, in response to GPR40 activation in the presence of indomethacin GSIS was inhibited (Fig. 7E). Based on its structure, it was possible that indomethacin might act as an antagonist of GPR40. To investigate this possibility we employed a Bioluminescence Resonance Energy Transfer (BRET) based β-arrestin-2 interaction assay detecting the interaction between mouse GPR40 and β-arrestin-2 (32). As predicted, addition of TUG469 potently increased GPR40-β-arrestin-2 interaction. However, indomethacin did not antagonize TUG469 activation of GPR40; rather, indomethacin behaved like a low potency agonist of GPR40 (EC_{50}= 4.5 ± 1.3 μM) acting additive at submaximal concentrations of TUG469 (Fig. 7F). Taken together, these results indicate that indomethacin in combination of fatty acid-dependent activation of GPR40 impair GSIS, which at least in part may explain the lack of a compensatory increase in GSIS to cope with the sustained hepatic glucose output in HF/HS+INDO fed mice.

DISCUSSION

In this study we report that HF/HS diet-induced obesity, GSIS and insulin resistance, but not glucose intolerance in C57BL/6J mice was prevented by the general COX inhibitor, indomethacin. In addition, fatty acid-dependent upregulation of GSIS was perturbed in HF/HS+INDO fed mice. Together, our findings point to a complex network controlling glucose tolerance and insulin secretion regulated by an intricate relationship between HF/HS feeding and indomethacin supplementation, where the lack of a compensatory upregulation of GSIS in combination with sustained elevated hepatic gluconeogenesis resulted in a state of glucose intolerance in the otherwise lean and insulin sensitive INDO supplemented mice.

Indomethacin prevented increased adipose tissue mass and hypertrophy induced by a HF/HS diet in C57BL/6J mice. This is in striking contrast to the obesity promoting action of indomethacin together with a HF/FS diet in Sv129 mice, normally considered obesity resistant (8).

High concentration of indomethacin has previously been reported to enhance PPARγ dependent transactivation, and thereby increase adipocyte differentiation (34,35). However, the

dose of indomethacin used in the present study was low (16mg per kg diet) compared to other studies considered insufficient to raise plasma levels sufficiently high to activate PPARγ, and accordingly, expression of PPARγ and PPARγ responsive genes in adipose tissues was not significantly altered comparing indomethacin supplemented and not supplemented mice (data not shown).

The effects of PGs in lipolysis are complex. It has been shown that lipolysis is reciprocally affected by PGE2 and PGI2, and possibly also modulated by other PGs (36). Exogenous PGE2 has been shown to reduce lipolysis, while PGI2 have been shown to antagonize the anti-lipolytic effect of PGE2. Inhibition of PGH synthesis by indomethacin reduce production of both PGE2 and PGI2, and in agreement with (36), thelevels of plasma glycerol and FFA in the fed state indicate that indomethacin did not seem to affect lipolysis (Fig. 2I). On the other hand, our results demonstrate that mice treated with indomethacin had a significant increase in plasma FFA after 16 hours fasting. In part, this might at least in part reflect an increased ability of fasting-induced increases in cAMP levels to promote lipolysis in the absence of inhibitory prostaglandins, and additionally, indomethacin might change the balance between lipolysis promoting and antagonizing PGs.
The observed protection against diet-induced obesity was associated with significantly reduced feed efficiency and weight gain, but surprisingly, this was not accompanied by detectable changes in O_2 consumption or CO_2 production. However, we cannot exclude the possibility that O_2 consumption and CO_2 production might be affected at a different time points during the experiment.

Insulin resistance is associated not only with obesity, but also low-grade inflammation in the adipose tissue (1,2), ectopic fat accumulation and increased DAG accumulation in both liver and skeletal muscle (37). COX-2 is necessary for the acute inflammatory response (38) and COX-2 deficiency attenuates age-dependent inflammation and infiltration of macrophages in adipose tissue (39). In the present study, inclusion of indomethacin reduced the circulating levels of 6-keto $PGF_{1\alpha}$, PGD_2, and TXB2 and reduced expression of markers of macrophage infiltration and inflammation in adipose tissues. Furthermore, indomethacin supplementation abolished HF/HS-induced accumulation of TAG and DAG in liver and muscle. Reflecting their lean phenotype and suppressed expression of inflammatory markers in adipose tissue, the HF/HS+INDO fed mice remained insulin sensitive. However, they developed glucose intolerance within one week of feeding.

Similar to the obese HF/HS fed mice, mice fed HF/HS+INDO had elevated sustained expression of genes involved in hepatic gluconeogenesis, suggesting a sustained high hepatic glucose output, correlated with high fasting and fed plasma glucose. This suggests a certain degree of insulin resistance in the liver, which however was undetectable in the HF/HS+INDO fed mice using whole body ITT. A hyperinsulinemic-euglycemic clamp experiment would be needed to draw a firm conclusion on the precise contribution of hepatic glucose output to the observed hyperglycemia. Nevertheless, our PTT data convincingly demonstrated that hepatic glucose output was increased in both obese HF/HS and lean HF/HS+INDO fed mice, and the early development of glucose intolerance in the lean HF/HS+INDO fed mice indicated that these mice in spite of being insulin sensitive were unable to compensate for the increased glucose output during a GTT.

HF/HS fed mice exhibited the expected correlation between obesity and hyperinsulinemia. By contrast, plasma insulin levels in the lean HF/HS+INDO fed mice were comparable to RD mice. These differences impinge on the important question as to whether hyperinsulinemia is a compensatory action to counteract obesity-elicited inflammation and peripheral insulin resistance or whether increased plasma insulin precedes obesity development, inflammation and insulin resistance. Whereas the canonical view favors the first possibility (1,40), others and we have recently argued that a high level of insulin is a prerequisite for HF-diet-induced obesity (41-43). In keeping with this view, adipose-specific insulin receptor knockout mice are protected against diet-induced obesity (44). Thus, the leanness of the HF/HS+INDO fed mice may

reflect a similar dependency on high insulin levels to elicit the obesogenic action of the HF/HS diet. High plasma insulin levels also exerts a positive feedback on β-cell mass expansion in response to HF/HS feeding, and similarly, the effect of glucose on β-cells may well depend on the increased insulin secretion. Accordingly, β-cell mass expansion and insulin hyper-secretion may eventually result in systemic insulin resistance (42,45).
The paradoxical situation of glucose intolerance in insulin sensitive mice developed only in the context of HF/HS feeding. This observation invited speculations that indomethacin in combination with a HF/HS diet perturbed the normal regulation of insulin synthesis and/or secretion from β-cells. Our finding that compared with HF/HS fed mice, mice fed HF/HS+INDO had decreased fasting and fed insulin levels and a reduced insulin secretion during a GTT suggested that indomethacin impaired HF/HS-induced GSIS.

Initially, the regulatory effect of fatty acids on GSIS was assumed to be related to fatty acid metabolism in β-cells, but now it is known that a large part of the effect depends on fatty acid activation of GPR40 (31). Using MIN6 cell as a model we demonstrated that the combined action of a selective GPR40 agonist, TUG469, and indomethacin inhibited GSIS. The augmented GSIS in HF fed C57BL/6 mice in response to *i.p*. glucose injection is reported to require GPR40 (32). In line with the finding that indomethacin does not influence GSIS in RD fed mice, GSIS is also unaffected in RD fed GPR40$^{-/-}$ C57BL/6 mice (32). Thus, although indomethacin did not act as a GRP40 antagonist, the finding that the combined action of indomethacin and TUG469 inhibited GSIS in MIN6 cells, suggests a mechanism by which indomethacin attenuates the compensatory increased insulin secretion in HF/HS fed mice.

In conclusion, our results demonstrate that indomethacin, a commonly used COX inhibitor, prevented HF/HS-induced obesity and insulin resistance, but not glucose intolerance and increased hepatic glucose production associated with a HF/HS diet. Indomethacin did not *per se* inhibit insulin secretion, but the indomethacin in combination with activation inhibited GSIS. In a situation of sustained hepatic glucose output, the inhibition of fatty acid enhancement of GSIS created a situation where pancreatic insulin secretion became insufficient to fully handle the glucose challenge of a GTT. Remaining important questions concern elucidating the precise molecular mechanisms by which indomethacin in combination with GPR40 activation inhibits GSIS and whether the effects of indomethacin and other NSAIDS can be translated into a human setting. Considering the worldwide common use of NSAIDS this question warrants further investigation.

Acknowledgments

We thank Trond Ulven for providing TUG469. We would also thank Pavel Flachs and Jan Kopecky for kindly providing the UCP1 antibody. This work was supported by the EU FP7 project DIABAT (HEALTH-F2-2011-278373), the Danish Natural Science Research Council, the Novo Nordisk Foundation, the Carlsberg Foundation, the SHARE Cross Faculty PhD Initiative of University of Copenhagen and NIFES. Part of the work was carried out as a part of the research program of the Danish Obesity Research Centre (DanORC). DanORC is supported by the Danish Council for Strategic Research (Grant No: 2101 06 0005). Part of the work was also supported by the Danish Council for Strategic Research (grant 11-116196 for the FFARMED project). The F.G.H laboratory receives funding from Juvenile Diabetes Research Foundation (1-2009-337) and NIH (RO1DK090492). This study was supported in part by intramural funds from the USDA Agricultural Research Service [5306-51000-002-00D to JWN; 5306-51000-019-00D to JWN] and the National Institute of Food and Agriculture National Needs Fellowship [2008-38420-04759 to AHK].

Author contributions

E.F., K.K., L.M. designed research. E.F., U.L.A., K.R., A.H.K., T.A., K.B., D.M.K., G.W.N., T.M., B.D.H., G.M., X.Y., J.W.N., F.G.H., B.L., K.K., L.M. conducted research and analyzed data. E.F., K.K., L.M. wrote the manuscript. All authors critically revised and approved the final content of the manuscript.

REFERENCES

1. Johnson, A. M. F., and Olefsky, J. M. (2013) The Origins and Drivers of Insulin Resistance. *Cell* **152**, 673-684
2. Donath, M. Y., and Shoelson, S. E. (2011) Type 2 diabetes as an inflammatory disease. *Nat Rev Immunol* **11**, 98-107
3. Robertson, R. P. (1998) Dominance of cyclooxygenase-2 in the regulation of pancreatic islet prostaglandin synthesis. *Diabetes* **47**, 1379-1383
4. Fujita, H., Kakei, M., Fujishima, H., Morii, T., Yamada, Y., Qi, Z., and Breyer, M. D. (2007) Effect of selective cyclooxygenase-2 (COX-2) inhibitor treatment on glucose-stimulated insulin secretion in C57BL/6 mice. *Biochem Biophys Res Commun* **363**, 37-43
5. Pereira Arias, A. M., Romijn, J. A., Corssmit, E. P., Ackermans, M. T., Nijpels, G., Endert, E., and Sauerwein, H. P. (2000) Indomethacin decreases insulin secretion in patients with type 2 diabetes mellitus. *Metabolism* **49**, 839-844
6. Topol, E., and Brodows, R. G. (1980) Effects of indomethacin on acute insulin release in man. *Diabetes* **29**, 379-382
7. Madsen, L., Pedersen, L. M., Liaset, B., Ma, T., Petersen, R. K., van den Berg, S., Pan, J., Muller-Decker, K., Dulsner, E. D., Kleemann, R., Kooistra, T., Doskeland, S. O., and Kristiansen, K. (2008) cAMP-dependent signaling regulates the adipogenic effect of n-6 polyunsaturated fatty acids. *J Biol Chem* **283**, 7196-7205
8. Madsen, L., Pedersen, L. M., Lillefosse, H. H., Fjaere, E., Bronstad, I., Hao, Q., Petersen, R. K., Hallenborg, P., Ma, T., De Matteis, R., Araujo, P., Mercader, J., Bonet, M. L., Hansen, J. B., Cannon, B., Nedergaard, J., Wang, J., Cinti, S., Voshol, P., Doskeland, S. O., and Kristiansen, K. (2010) UCP1 induction during recruitment of brown adipocytes in white adipose tissue is dependent on cyclooxygenase activity. *PLoS One* **5**, e11391
9. Vegiopoulos, A., Muller-Decker, K., Strzoda, D., Schmitt, I., Chichelnitskiy, E., Ostertag, A., Berriel Diaz, M., Rozman, J., Hrabe de Angelis, M., Nusing, R. M., Meyer, C. W., Wahli, W., Klingenspor, M., and Herzig, S. (2010) Cyclooxygenase-2 controls energy homeostasis in mice by de novo recruitment of brown adipocytes. *Science* **328**, 1158-1161
10. Andrikopoulos, S., Blair, A. R., Deluca, N., Fam, B. C., and Proietto, J. (2008) Evaluating the glucose tolerance test in mice. *American Journal of Physiology - Endocrinology And Metabolism* **295**, E1323-E1332
11. Wan, S. G., Taccioli, C., Jiang, Y., Chen, H., Smalley, K. J., Huang, K., Liu, X. P., Farber, J. L., Croce, C. M., and Fong, L. Y. (2011) Zinc deficiency activates S100A8 inflammation in the absence of COX-2 and promotes murine oral-esophageal tumor progression. *Int J Cancer* **129**, 331-345
12. Liaset, B., Hao, Q., Jørgensen, H., Hallenborg, P., Du, Z.-Y., Ma, T., Marschall, H.-U., Kruhøffer, M., Li, R., Li, Q., Yde, C. C., Criales, G., Bertram, H. C., Mellgren, G., Øfjord, E. S., Lock, E.-J., Espe, M., Frøyland, L., Madsen, L., and Kristiansen, K. (2011) Nutritional Regulation of Bile Acid Metabolism Is Associated with Improved Pathological Characteristics of the Metabolic Syndrome. *Journal of Biological Chemistry* **286**, 28382-28395
13. Luria, A., Bettaieb, A., Xi, Y., Shieh, G. J., Liu, H. C., Inoue, H., Tsai, H. J., Imig, J. D., Haj, F. G., and Hammock, B. D. (2011) Soluble epoxide hydrolase deficiency alters pancreatic islet size and improves glucose homeostasis in a model of insulin resistance. *Proc Natl Acad Sci U S A* **108**, 9038-9043

14. Christiansen, E., Due-Hansen, M. E., Urban, C., Merten, N., Pfleiderer, M., Karlsen, K. K., Rasmussen, S. S., Steensgaard, M., Hamacher, A., Schmidt, J., Drewke, C., Petersen, R. K., Kristiansen, K., Ullrich, S., Kostenis, E., Kassack, M. U., and Ulven, T. (2010) Structure−Activity Study of Dihydrocinnamic Acids and Discovery of the Potent FFA1 (GPR40) Agonist TUG-469. *ACS Medicinal Chemistry Letters* **1**, 345-349
15. Malaisse, W. J., Zhang, Y., Louchami, K., Sharma, S., Dresselaers, T., Himmelreich, U., Novotny, G. W., Mandrup-Poulsen, T., Waschke, D., Leshch, Y., Thimm, J., Thiem, J., and Sener, A. (2012) 19F-heptuloses as tools for the non-invasive imaging of GLUT2-expressing cells. *Archives of Biochemistry and Biophysics* **517**, 138-143
16. Christiansen, E., Hansen, S. V., Urban, C., Hudson, B. D., Wargent, E. T., Grundmann, M., Jenkins, L., Zaibi, M., Stocker, C. J., Ullrich, S., Kostenis, E., Kassack, M. U., Milligan, G., Cawthorne, M. A., and Ulven, T. (2013) Discovery of TUG-770: A Highly Potent Free Fatty Acid Receptor 1 (FFA1/GPR40) Agonist for Treatment of Type 2 Diabetes. *ACS Med Chem Lett* **4**, 441-445
17. Katsuki, A., Sumida, Y., Gabazza, E. C., Murashima, S., Furuta, M., Araki-Sasaki, R., Hori, Y., Yano, Y., and Adachi, Y. (2001) Homeostasis model assessment is a reliable indicator of insulin resistance during follow-up of patients with type 2 diabetes. *Diabetes Care* **24**, 362-365
18. Katz, A., Nambi, S. S., Mather, K., Baron, A. D., Follmann, D. A., Sullivan, G., and Quon, M. J. (2000) Quantitative insulin sensitivity check index: a simple, accurate method for assessing insulin sensitivity in humans. *J Clin Endocrinol Metab* **85**, 2402-2410
19. Lillefosse, H. H., Tastesen, H. S., Du, Z. Y., Ditlev, D. B., Thorsen, F. A., Madsen, L., Kristiansen, K., and Liaset, B. (2013) Hydrolyzed Casein Reduces Diet-Induced Obesity in Male C57BL/6J Mice. *J Nutr*
20. Liaset, B., Julshamn, K., and Espe, M. (2003) Chemical composition and theoretical nutritional evaluation of the produced fractions from enzymic hydrolysis of salmon frames with Protamex (TM). *Process Biochem* **38**, 1747-1759
21. Stephensen, C. B., Armstrong, P., Newman, J. W., Pedersen, T. L., Legault, J., Schuster, G. U., Kelley, D., Vikman, S., Hartiala, J., Nassir, R., Seldin, M. F., and Allayee, H. (2011) ALOX5 gene variants affect eicosanoid production and response to fish oil supplementation. *J Lipid Res* **52**, 991-1003
22. Keenan, A. H., Pedersen, T. L., Fillaus, K., Larson, M. K., Shearer, G. C., and Newman, J. W. (2012) Basal omega-3 fatty acid status affects fatty acid and oxylipin responses to high-dose n3-HUFA in healthy volunteers. *Journal of Lipid Research* **53**, 1662-1669
23. Dikopoulos, N., Schmid, R. M., Bachem, M., Buttenschoen, K., Adler, G., Chiang, J. Y., and Weidenbach, H. (2007) Bile synthesis in rat models of inflammatory bowel diseases. *Eur J Clin Invest* **37**, 222-230
24. Yamamoto, F. (1980) Contribution of prostaglandin to the contraction induced by catecholamines in the isolated gallbladder of the guinea-pig. *Gastroenterol Jpn* **15**, 433-438
25. Richelsen, B., and Pedersen, S. B. (1987) Antilipolytic Effect of Prostaglandin E2 in Perifused Rat Adipocytes. *Endocrinology* **121**, 1221-1226
26. Heilbronn, L. K., and Campbell, L. V. (2008) Adipose tissue macrophages, low grade inflammation and insulin resistance in human obesity. *Curr Pharm Des* **14**, 1225-1230
27. Nagle, C. A., Klett, E. L., and Coleman, R. A. (2009) Hepatic triacylglycerol accumulation and insulin resistance. *J Lipid Res* **50**, S74-S79

28. Montell, E., Turini, M., Marotta, M., Roberts, M., Noe, V., Ciudad, C. J., Mace, K., and Gomez-Foix, A. M. (2001) DAG accumulation from saturated fatty acids desensitizes insulin stimulation of glucose uptake in muscle cells. *Am J Physiol Endocrinol Metab* **280**, E229-237
29. Erion, D. M., and Shulman, G. I. (2010) Diacylglycerol-mediated insulin resistance. *Nature Medicine* **16**, 400-402
30. Poitout, V. (2013) Lipotoxicity impairs incretin signalling. *Diabetologia* **56**, 231-233
31. Mancini, A. D., and Poitout, V. (2013) The fatty acid receptor FFA1/GPR40 a decade later: how much do we know? *Trends in Endocrinology & Metabolism* **24**, 398-407
32. Kebede, M., Alquier, T., Latour, M. G., Semache, M., Tremblay, C., and Poitout, V. (2008) The fatty acid receptor GPR40 plays a role in insulin secretion in vivo after high-fat feeding. *Diabetes* **57**, 2432-2437
33. Forman, B. M., Tontonoz, P., Chen, J., Brun, R. P., Spiegelman, B. M., and Evans, R. M. (1995) 15-Deoxy-delta 12, 14-prostaglandin J2 is a ligand for the adipocyte determination factor PPAR gamma. *Cell* **83**, 803-812
34. Brown, P. J., Smith-Oliver, T. A., Charifson, P. S., Tomkinson, N. C., Fivush, A. M., Sternbach, D. D., Wade, L. E., Orband-Miller, L., Parks, D. J., Blanchard, S. G., Kliewer, S. A., Lehmann, J. M., and Willson, T. M. (1997) Identification of peroxisome proliferator-activated receptor ligands from a biased chemical library. *Chem Biol* **4**, 909-918
35. Jaradat, M. S., Wongsud, B., Phornchirasilp, S., Rangwala, S. M., Shams, G., Sutton, M., Romstedt, K. J., Noonan, D. J., and Feller, D. R. (2001) Activation of peroxisome proliferator-activated receptor isoforms and inhibition of prostaglandin H(2) synthases by ibuprofen, naproxen, and indomethacin. *Biochem Pharmacol* **62**, 1587-1595
36. Chatzipanteli, K., Rudolph, S., and Axelrod, L. (1992) Coordinate control of lipolysis by prostaglandin E2 and prostacyclin in rat adipose tissue. *Diabetes* **41**, 927-935
37. Bonen, A., Parolin, M. L., Steinberg, G. R., Calles-Escandon, J., Tandon, N. N., Glatz, J. F., Luiken, J. J., Heigenhauser, G. J., and Dyck, D. J. (2004) Triacylglycerol accumulation in human obesity and type 2 diabetes is associated with increased rates of skeletal muscle fatty acid transport and increased sarcolemmal FAT/CD36. *Faseb J* **18**, 1144-1146
38. Seibert, K., and Masferrer, J. L. (1994) Role of inducible cyclooxygenase (COX-2) in inflammation. *Receptor* **4**, 17-23
39. Ghoshal, S., Trivedi, D. B., Graf, G. A., and Loftin, C. D. (2011) Cyclooxygenase-2 deficiency attenuates adipose tissue differentiation and inflammation in mice. *J Biol Chem* **286**, 889-898
40. Saltiel, A. R. (2012) Insulin Resistance in the Defense against Obesity. *Cell metabolism* **15**, 798-804
41. Hao, Q., Lillefosse, H. H., Fjaere, E., Myrmel, L. S., Midtbo, L. K., Jarlsby, R. H., Ma, T., Jia, B., Petersen, R. K., Sonne, S. B., Chwalibog, A., Froyland, L., Liaset, B., Kristiansen, K., and Madsen, L. (2012) High-glycemic index carbohydrates abrogate the antiobesity effect of fish oil in mice. *Am J Physiol Endocrinol Metab* **302**, E1097-1112
42. Mehran, A. E., Templeman, N. M., Brigidi, G. S., Lim, G. E., Chu, K. Y., Hu, X. K., Botezelli, J. D., Asadi, A., Hoffman, B. G., Kieffer, T. J., Bamji, S. X., Clee, S. M., and Johnson, J. D. (2012) Hyperinsulinemia Drives Diet-Induced Obesity Independently of Brain Insulin Production. *Cell metabolism* **16**, 723-737
43. Brons, C., Jensen, C. B., Storgaard, H., Hiscock, N. J., White, A., Appel, J. S., Jacobsen, S., Nilsson, E., Larsen, C. M., Astrup, A., Quistorff, B., and Vaag, A.

(2009) Impact of short-term high-fat feeding on glucose and insulin metabolism in young healthy men. *J Physiol-London* **587**, 2387-2397

44. Bluher, M., Michael, M. D., Peroni, O. D., Ueki, K., Carter, N., Kahn, B. B., and Kahn, C. R. (2002) Adipose tissue selective insulin receptor knockout protects against obesity and obesity-related glucose intolerance. *Dev Cell* **3**, 25-38
45. Okada, T., Liew, C. W., Hu, J., Hinault, C., Michael, M. D., Krutzfeldt, J., Yin, C., Holzenberger, M., Stoffel, M., and Kulkarni, R. N. (2007) Insulin receptors in beta-cells are critical for islet compensatory growth response to insulin resistance. *P Natl Acad Sci USA* **104**, 8977-8982
46. Steneberg, P., Rubins, N., Bartoov-Shifman, R., Walker, M. D., and Edlund, H. (2005) The FFA receptor GPR40 links hyperinsulinemia, hepatic steatosis, and impaired glucose homeostasis in mouse. *Cell Metab* **1**, 245-258
47. Lan, H., Hoos, L. M., Liu, L., Tetzloff, G., Hu, W., Abbondanzo, S. J., Vassileva, G., Gustafson, E. L., Hedrick, J. A., and Davis, H. R. (2008) Lack of FFAR1/GPR40 does not protect mice from high-fat diet-induced metabolic disease. *Diabetes* **57**, 2999-3006

FIGURE LEGENDS

FIGURE 1: Effect of indomethacin supplementation on body weight gain and adipose tissue mass. Mice were fed RD, HF/HS or HF/HS+INDO for 7 weeks. The mice were killed and liver and adipose tissue depots were dissected out and weighted. (A) Body weight development during 7 weeks of feeding. (B) Mean total body weight gain after 7 weeks of feeding. (C) Mean weight of eWAT (epididymal white adipose tissue), rWAT (retroperitoneal white adipose tissue), and iWAT (inguinal white adipose tissue). (D) Mean liver weight. (E) Mean weight of iBAT (interscapular brown adipose tissue). (F) Total energy intake calculated from the amount of food eaten during the experiment. (G) Energy efficiency calculated as weight gain relative to Megajoule (kJ). (H) Feces were collected for 48 hours and the fat content measured to estimate percentage fat absorption. (I) Total percentage weight loss after 12 hours starvation in mice treated with the respective diets. All results are presented as mean + SEM (n=8-9). Statistical significances are denoted with stars; * $P \leq 0.05$, ** $P \leq 0.01$, *** $P \leq 0.001$.

FIGURE 2: The effect of indomethacin on metabolic performance, expression of markers of brown and brown-like adipocytes, and plasma levels of glycerol, NEFA, alanine aminotransferase (ALT), and aspartate transaminase (AST) after 7 weeks of feeding. Mice fed RD, HF/HS and HF/HS+INDO were placed in open circuit chamber for 24 hours for measurements of O_2 consumption and CO_2 production. (A and B) O_2 uptake and production CO_2 expressed as ml/h/kg. (C) Calculation of respiration exchange ratio (RER). (D-F) mRNA levels of markers of brown and brown-like adipocytes in iBAT, eWAT and iWAT. *Ucp1* (Uncoupling protein 1), *Dio2* (Deiodinase, iodothyronine, type II), *Ppargc1a* (Peroxisome proliferator-activated receptor gamma, coactivator 1 alpha). (G) Immunohistochemistry (IHC) staining with UCP1-antibody for detection of multilocular cells in representative sections from eWAT and iWAT. (H) Plasma levels of ALT measured in the fed state and AST measured in the fasted state (12h). (I) Plasma glycerol levels in fed and fasted mice. (J) Plasma levels of NEFA in the fed and the fasted state. The results are presented as mean + SEM (n=8-9). Statistical significances are denoted with stars; * $P \leq 0.05$, ** $P \leq 0.01$, *** $P \leq 0.001$.

FIGURE 3: Effects of indomethacin supplementation on adipocyte morphology and inflammation. (A) Morphology of eWAT and iWAT from mice fed RD, HF/HS and HF/HS+INDO for 7 weeks (n=3). The tissues were stained with hematoxylin-eosin. Micrographs from one representative mouse in each group is shown. (B-I) Quantitative real-time RT-PCR analysis of markers of macrophage infiltration and inflammation in eWAT (B-E) and iWAT. *Cd68* (Cluster of differentiation 68), *Emr1* (Egf-like module containing, mucin-like, hormone receptor-like 1), *Serpine1* (Serpin peptidase inhibitor, clade E, member 1), *Ccl2* (Chemokine ligand 2) (F-I). (J) Immunohistochemistry (IHC) staining with F4/80-antibody for detection of macrophages and Crown-like structures (CLS) in representative sections from eWAT and iWAT. The results are presented as mean + SEM (n=8-9). Statistical significances are denoted with stars; ** $P \leq 0.01$, *** $P \leq 0.001$.

FIGURE 4: Effects of indomethacin supplementation on lipid accumulation in liver and muscle and insulin sensitivity. Quantitative analyses of lipids in the liver and muscle of mice fed RD, HF/HS and HF/HS+INDO for 7 weeks were performed (n=8-9). (A) Triacylglycerol (TAG) and (B) diacylglycerol (DAG) in liver. (C) TAG and (D) DAG in tibialis anterior muscle. (E) HOMA-IR calculated from fasting plasma (12h) levels of insulin and glucose. (F) QUICKI (G) ITT after 6 weeks on the respective diets. Blood glucose from RD fed mice were significantly different from mice given a HF/HS diet at timepoint 15, 30, 45 and 60 after injection, but is not shown in figure. All results are presented as mean + SEM (n=8-9). Statistical significances are denoted with stars; * $P \leq 0.05$, ** $P \leq 0.01$, *** $P \leq 0.001$.

FIGURE 5: Effects of indomethacin supplementation on glucose tolerance, insulin sensitivity, hepatic glucose production and glucose-stimulated insulin secretion. (A) Plasma blood glucose levels in fed and 12 hours fasted animals after 7 weeks of feeding. (B) Intraperitoneal glucose tolerance test (2g/kg) performed on mice fasted for 6 hours. (C) GSIS during GTT after 7 weeks treatment with the respective diets. (C) PTT after 6 weeks of feeding with a RD, HF/HS and the

HF/HS+INDO diet. (D-E) mRNA levels of *G6pc* (Glucose-6-phosphatase) and *Pck1* (Phosphoenolpyruvate carboxykinase 1) in liver in the fed state. The results are presented as mean + SEM (n=8-9). (G-H) GTT and GSIS after 1 week on the respective diets. (I-J) GTT and GSIS after 2 weeks. (K-L) GTT and GSIS after 3 weeks. Statistical significances are denoted with stars; * P≤0.05, ** P≤0.01, *** P≤0.00

FIGURE 6: Effects of acute COX-inhibition with indomethacin, indomethacin combined in a balanced RD diet and indomethacin supplementation to already obese animals. (A-C) Acute effects of indomethacin on GTT and GSIS in C57BL/6J mice given an RD diet for 1 week. The mice were given indomethacin (2.5 mg/kg-BW) orally 1 hour before a glucose tolerance test during which GSIS was also evaluated. (D-F) Acute effects of indomethacin on glucose tolerance and GSIS in mice fed a HF/HS diet for 10 weeks. (G) Weight of eWAT, rWAT and iWAT in mice fed RD and RD+INDO for 7 weeks. (H-I) GTT and GSIS after 6 weeks of feeding with RD supplemented with indomethacin. (J-O) Mice were fed RD or a HF/HS diet for 10 weeks, and then continued on either a HF/HS diet with or without indomethacin supplementation or the RD diet for additional 8 weeks. (J) BW, (K) feed efficiency, (L) lean body mass and (M) fat mass is shown for 6 weeks after changing the diet. (N-O) GTT and GSIS on the mice shown in J-M. The results are presented as mean + SEM (n=8-9). Statistical significances are denoted with stars; * P≤0.05, ** P≤0.01, *** P≤0.00

FIGURE 7: Effects of indomethacin supplementation on glucose-stimulated first phase insulin secretion in C57BL/6J mice, and TUG469 stimulated insulin secretion in MIN6 cells. (A) Plasma insulin levels in fed and 12 hours fasted animals after 8 weeks of feeding. (B) Pancreatic islet and section sizes were analyzed, and islet size as a percentage of total pancreas size was calculated (n=5). (C) First phase insulin secretion and glucose-stimulated insulin secretion measured after 3 hours fasting. (D) MIN6 cells treated with indomethacin at 0.1, 1 or 10uM. (E) MIN6 cells treated with vehicle, indomethacin (1μM), TUG469 or TUG469+INDO. After 1 hour incubation, insulin release was measured. (F) Effects of TUG469 and Indomethacin on β-arrestin-2 recruitment to mouse GPR40. BRET signals normalized to the maximal TUG469 response obtained following treatment with varying concentrations of TUG469 (blue) or INDO (red) on their own, or to varying concentrations of INDO in the presence of 100 nM TUG469 (green). The results are presented as mean + SEM (n=8-9). Statistical significances are denoted with stars; * P≤0.05, ** P≤0.01, *** P≤0.00

TABLE 1: Average plasma concentrations of oxylipin metabolites (nM). The levels of plasma oxylipids were determined by UPLC-MS/MS. Results are presented as mean ± SD (n=6). *P*-values were calculated by 2-tailed t-test. Statistical significances are denoted with stars; * P≤0.05, ** P≤0.001.

Analyte	Parent	Class	HF/HS	HF/HS + INDO	*p*-value*
PGD2	AA	Prostaglandin	0.376 ± 0.140	0.108 ± 0.086	**
PGF2a	AA	Prostaglandin	0.184 ± 0.0782	0.0667 ± 0.081	*
6-keto PGF1a	AA	Prostaglandin	0.537 ± 0.208	0.226 ± 0.1	**
TXB2	AA	Thromboxane	0.229 ± 0.195	n/d	*
12-HETE	AA	Alcohol	115 ± 75.4	117 ± 67	ns
11-HETE	AA	Alcohol	1.85 ± 1.82	2.88 ± 4.4	ns
9-HETE	AA	Alcohol	3.66 ± 3.26	5.12 ± 7.5	ns
8-HETE	AA	Alcohol	3.71 ± 3.03	5.53 ± 4.2	ns
5-HETE	AA	Alcohol	6.32 ± 7.26	6.88 ± 7.3	ns
15-HEPE	EPA	Alcohol	0.190 ± 0.138	0.204 ± 0.23	ns
12-HEPE	EPA	Alcohol	1.69 ± 1.59	1.24 ± 0.78	ns
15-HETrE	GLA	Alcohol	1.15 ± 1.04	1.94 ± 3	ns
13-HODE	LA	Alcohol	131 ± 51.0	177 ± 83	ns
9-HODE	LA	Alcohol	28.0 ± 12.9	29.2 ± 16	ns
9-HOTE	ALA	Alcohol	1.93 ± 0.258	1.8 ± 0.63	ns
13-HOTE	ALA	Alcohol	1.71 ± 0.281	1.52 ± 0.84	ns
15-KETE	AA	Ketone	4.32 ± 2.29	2.54 ± 0.76	ns
12-KETE	AA	Ketone	4.42 ± 2.32	2.72 ± 0.76	ns
5-KETE	AA	Ketone	2.97 ± 1.74	2.15 ± 1.6	ns
13-KODE	LA	Ketone	96.3 ± 80.1	95.5 ± 72	ns
12(13)-EpOME	LA	Epoxide	32.7 ± 9.41	29.9 ± 20	ns
15(16)-EpODE	ALA	Epoxide	2.16 ± 0.623	2.05 ± 1.2	ns
9(10)-EpODE	ALA	Epoxide	2.24 ± 0.847	2.66 ± 1.4	ns
14,15-DiHETrE	AA	Diol	1.49 ± 0.602	0.929 ± 0.13	ns
5,6-DiHETrE	AA	Diol	0.459 ± 0.117	0.412 ± 0.15	ns
17,18-DiHETE	EPA	Diol	2.67 ± 1.36	2.08 ± 0.86	ns
14,15-DiHETE	EPA	Diol	0.330 ± 0.108	0.213 ± 0.17	ns
19,20-DiHDPA	DHA	Diol	1.76 ± 0.731	1.36 ± 0.24	ns
9,10-DiHOME	LA	Diol	48.8 ± 19.2	51.1 ± 15	ns
9,10-DiHODE	ALA	Diol	0.189 ± 0.235	0.174 ± 0.22	ns
9,12,13-TriHOME	LA	Triol	3.35 ± 1.55	2.48 ± 1.3	ns
9,10-13-TriHOME	LA	Triol	1.48 ± 1.22	0.876 ± 0.68	ns

Fig.1

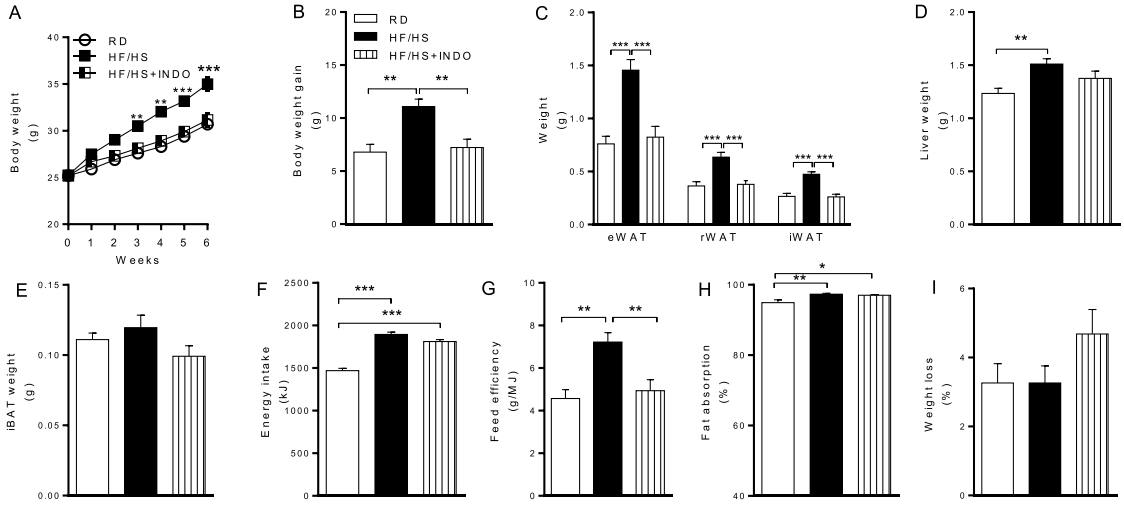
A
RD
HF/HS
HF/HS+INDO
Body weight (g)
Weeks
B
Body weight gain (g)
C
Weight (g)
eWAT
rWAT
iWAT
D
Liver weight (g)
E
iBAT weight (g)
F
Energy intake (kJ)
G
Feed efficiency (g/MJ)
H
Fat absorption (%)
I
Weight loss (%)

Fig.2

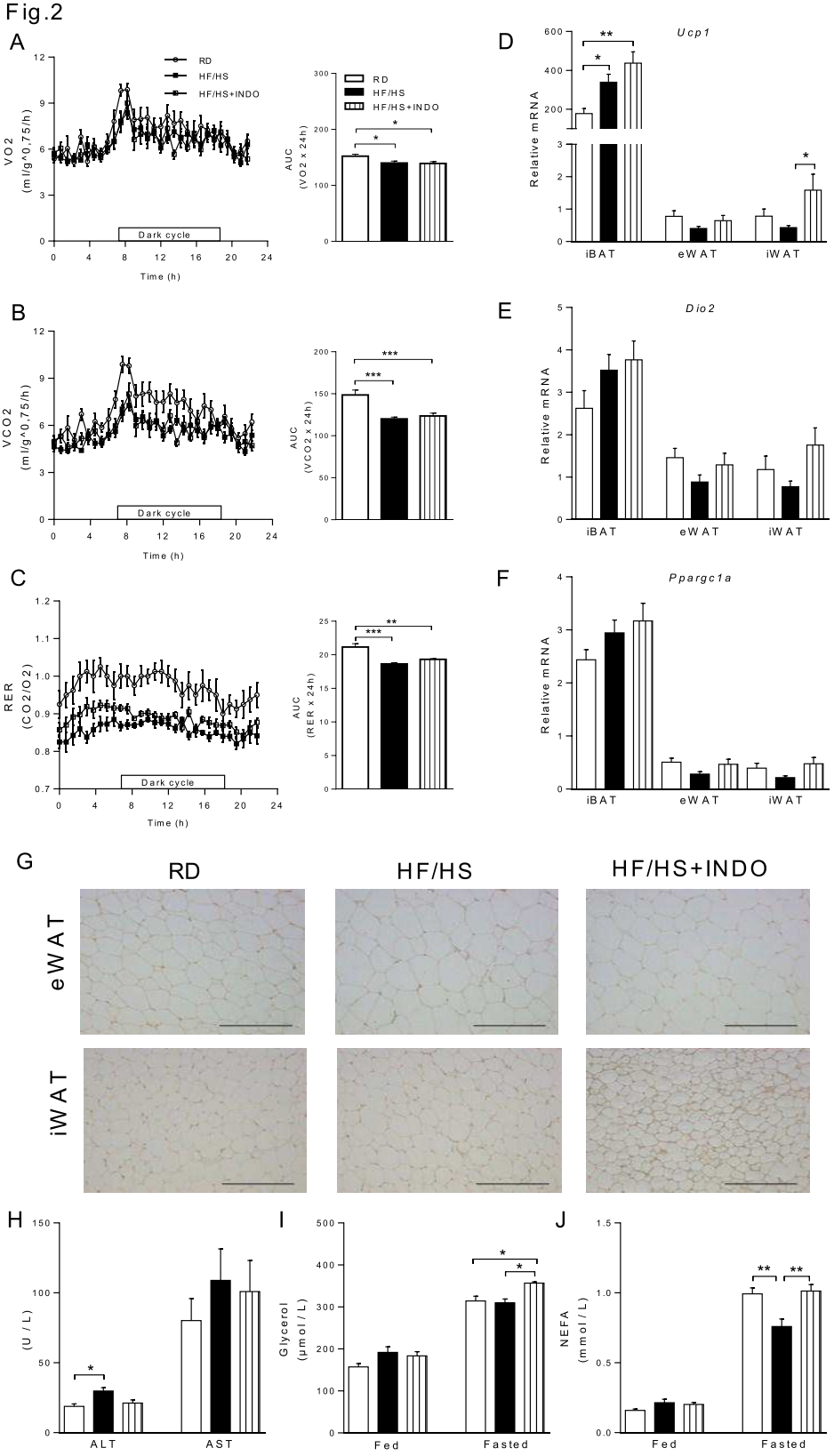
A
RD
HF/HS
HF/HS+INDO
VO2 (ml/g^0,75/h)
Dark cycle
Time (h)
AUC (VO2 x 24h)
B
VCO2 (ml/g^0,75/h)
AUC (VCO2 x 24h)
C
RER (CO2/O2)
AUC (RER x 24h)
D
Ucp1
Relative mRNA
iBAT
eWAT
iWAT
E
Dio2
F
Ppargc1a
G
RD
HF/HS
HF/HS+INDO
eWAT
iWAT
H
(U / L)
ALT
AST
I
Glycerol (µmol / L)
Fed
Fasted
J
NEFA (mmol / L)

Fig.3

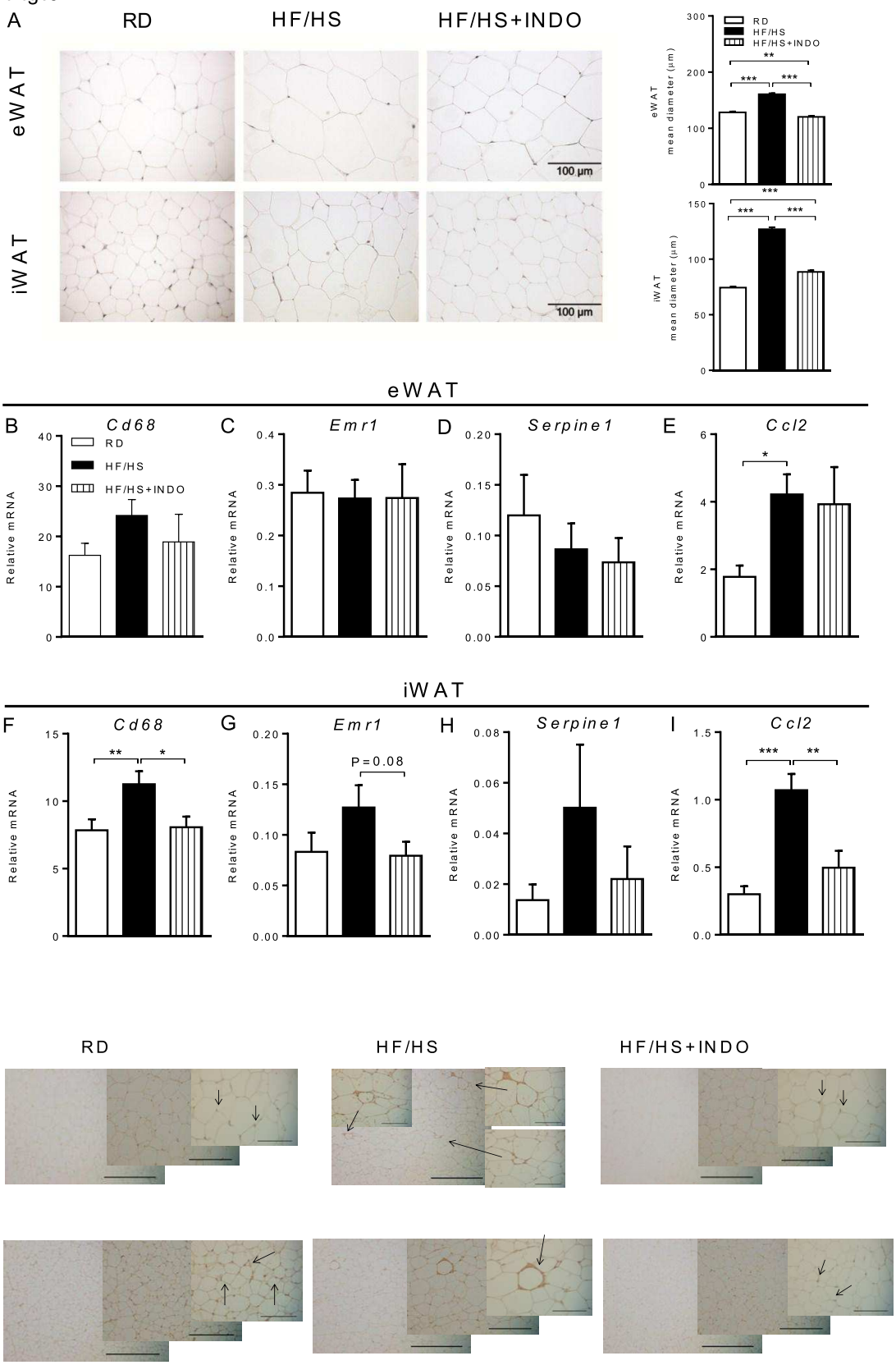
A
RD
HF/HS
HF/HS+INDO
eWAT
iWAT
100 μm
100 μm
RD
HF/HS
HF/HS+INDO
eWAT mean diameter (μm)
iWAT mean diameter (μm)
eWAT
B Cd68
C Emr1
D Serpine1
E Ccl2
Relative mRNA
iWAT
F Cd68
G Emr1
H Serpine1
I Ccl2
P=0.08
J
RD
HF/HS
HF/HS+INDO
eWAT
iWAT

Fig.4

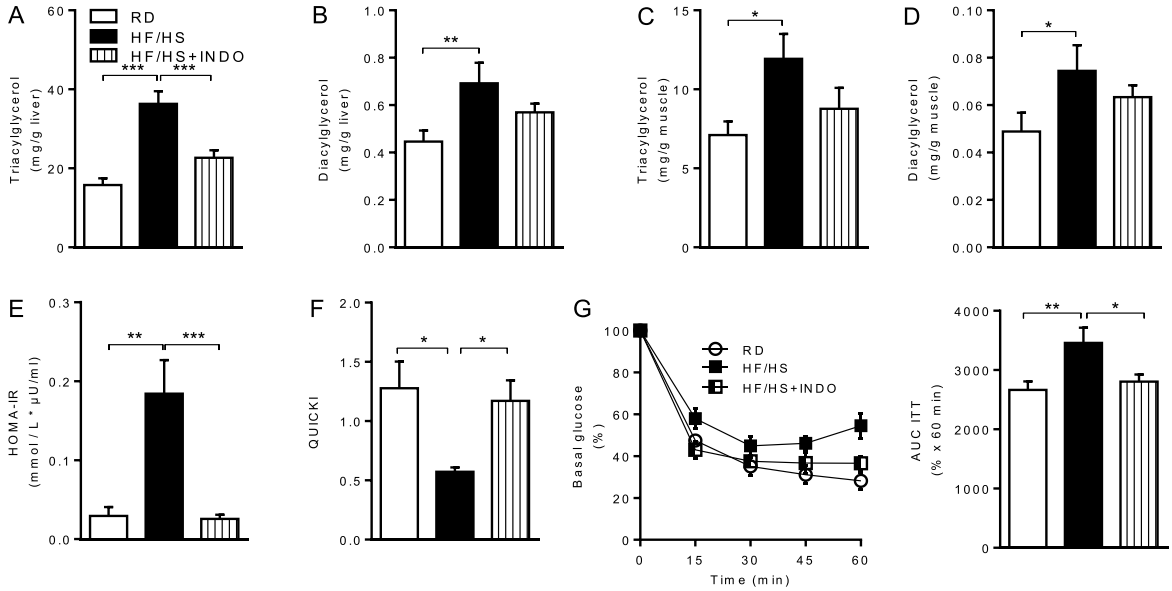
A
RD
HF/HS
HF/HS+INDO
Triacylglycerol (mg/g liver)
B
Diacylglycerol (mg/g liver)
C
Triacylglycerol (mg/g muscle)
D
Diacylglycerol (mg/g muscle)
E
HOMA-IR (mmol/L * μU/ml)
F
QUICKI
G
Basal glucose (%)
Time (min)
AUC ITT (% x 60 min)

Fig.5

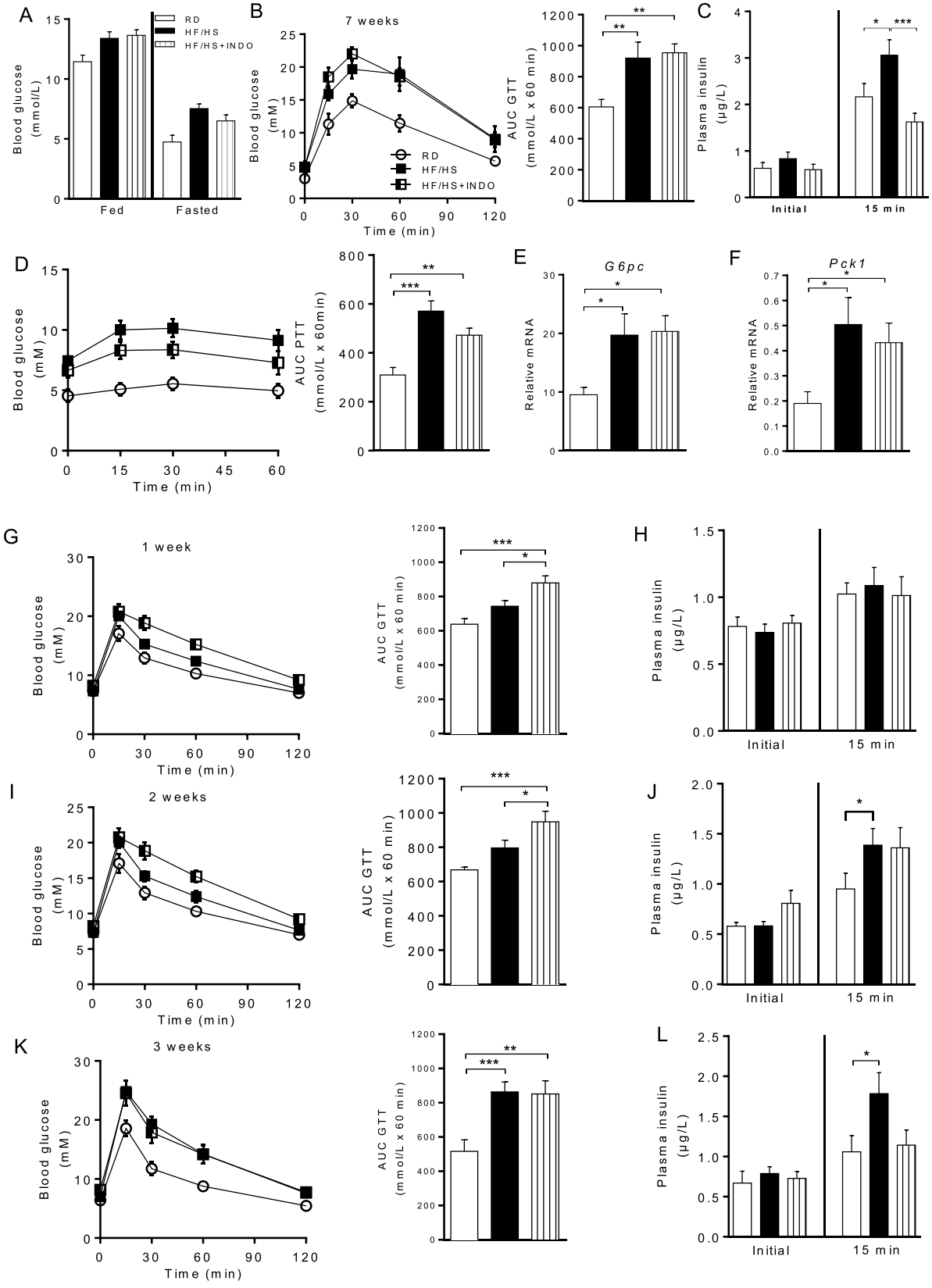
A
Blood glucose (mmol/L)
RD
HF/HS
HF/HS+INDO
Fed
Fasted
B
7 weeks
Blood glucose (mM)
Time (min)
AUC GTT (mmol/L x 60 min)
C
Plasma insulin (µg/L)
Initial
15 min
D
Blood glucose (mM)
Time (min)
AUC PTT (mmol/L x 60min)
E
G6pc
Relative mRNA
F
Pck1
Relative mRNA
G
1 week
H
I
2 weeks
J
K
3 weeks
L

Fig.6

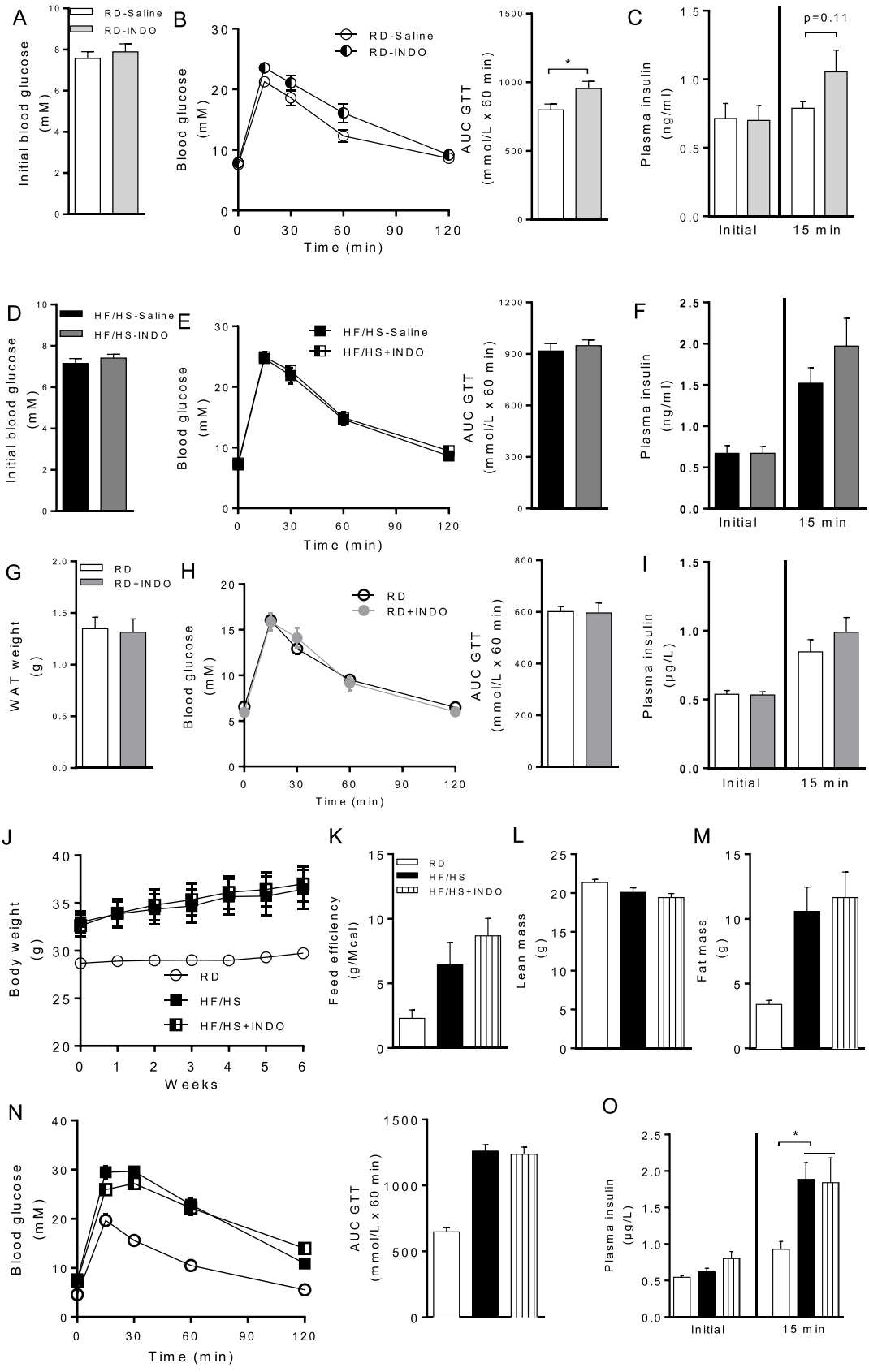
A
RD-Saline
RD-INDO
Initial blood glucose (mM)
B
RD-Saline
RD-INDO
Blood glucose (mM)
Time (min)
AUC GTT (mmol/L x 60 min)
*
C
p=0.11
Plasma insulin (ng/ml)
Initial
15 min
D
HF/HS-Saline
HF/HS-INDO
Initial blood glucose (mM)
E
HF/HS-Saline
HF/HS+INDO
Blood glucose (mM)
Time (min)
AUC GTT (mmol/L x 60 min)
F
Plasma insulin (ng/ml)
Initial
15 min
G
RD
RD+INDO
WAT weight (g)
H
RD
RD+INDO
Blood glucose (mM)
Time (min)
AUC GTT (mmol/L x 60 min)
I
Plasma insulin (µg/L)
Initial
15 min
J
Body weight (g)
RD
HF/HS
HF/HS+INDO
Weeks
K
RD
HF/HS
HF/HS+INDO
Feed efficiency (g/Mcal)
L
Lean mass (g)
M
Fat mass (g)
N
Blood glucose (mM)
Time (min)
AUC GTT (mmol/L x 60 min)
O
Plasma insulin (µg/L)
*
Initial
15 min

Fig.7

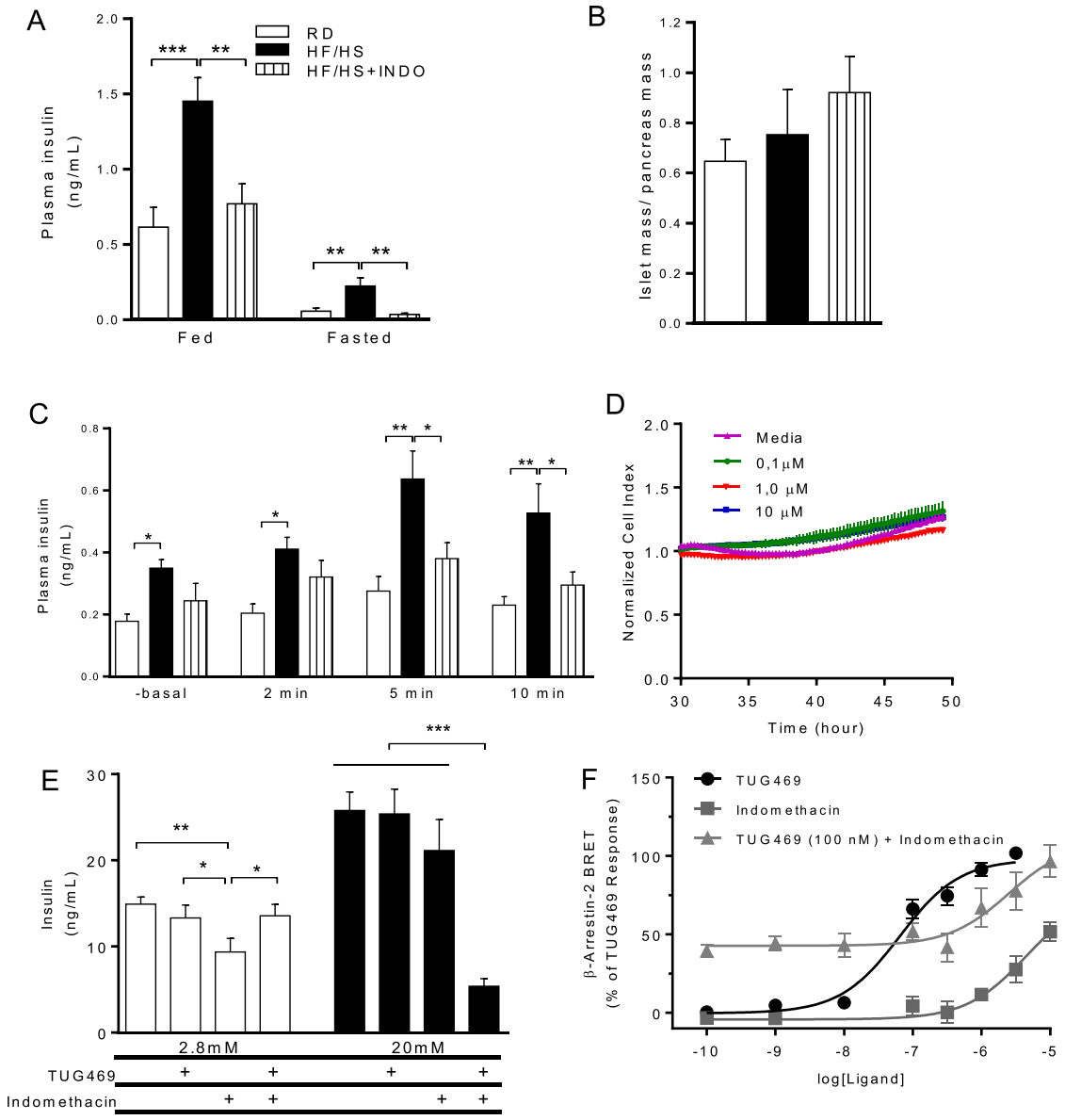
A
RD
HF/HS
HF/HS+INDO
Plasma insulin (ng/mL)
Fed
Fasted
B
Islet mass/ pancreas mass
C
Plasma insulin (ng/mL)
-basal
2 min
5 min
10 min
D
Media
0,1μM
1,0 μM
10 μM
Normalized Cell Index
Time (hour)
E
Insulin (ng/mL)
2.8mM
20mM
TUG469
Indomethacin
F
TUG469
Indomethacin
TUG469 (100 nM) + Indomethacin
β-Arrestin-2 BRET (% of TUG469 Response)
log[Ligand]